Biometals (2011) 24:663–677
DOI 10.1007/s10534-011-9419-4

Metabolomic profiles delineate potential roles for gadolinium chloride in the proliferation or inhibition of Hela cells

Xiao-Hui Long · Peng-Yuan Yang · Qiong Liu · Jun Yao · Yi Wang · Guo-Hua He · Guang-Yan Hong · Jia-Zuan Ni

Received: 21 October 2010 / Accepted: 22 January 2011 / Published online: 4 February 2011

Abstract Lanthanides (Lns) compounds have been reported to possess contrary effects on cell activity, i.e., promoting cell cycle progression and cell growth by lower concentration treatment, but suppressing cell proliferation and inducing cell apoptosis at higher dosing. However, the cellular processes during the intervention and the possible underlying mechanisms are still not well clarified. Using a combination of high-throughput liquid chromatography (LC) with mass spectrometry (MS), we have investigated the metabolomic profiles of Hela cells following gadolinium chloride ($GdCl_3$) treatment in time- and concentration- dependent manners. A total of 48 metabolites released by Hela cells are identified to be differentially expressed ($P < 0.05$) in different states. Metabolic pathways analyses reveal that the differential metabolites are mainly characterized by increased lipid and amino acid metabolisms and by decreased lipid, amino acid, and carbohydrate metabolisms for cells treated with $GdCl_3$ at lower and higher concentrations, respectively. Notably, in the higher level $GdCl_3$ case, the down-expressions of metabolites are predominantly in the glycolytic and the redox pathways. The above results, obtained by using a metabolomic strategy for the first time, disclose that different cell signaling pathways are activated by $GdCl_3$ treatment with different concentrations, leading to inhibitory or promotional effect on Hela cells.

Keywords Gadolinium chloride · Hela cells · Metabolomic profiling · Liquid chromatography-mass spectrometry · Cell growth

Introduction

Lns (rare earth metals) have a variety of physical or chemical properties, and have been widely investigated and applied in agriculture and medicine since twenty century (Ni 2002; Fricker 2006). As a member of Lns family, gadolinium (Gd) shows particularly multi-biological effects on organisms and attracts more and more interests of biochemists and clinicians. For example, clinically, chelates of gadolinium such as gadolinium diethylenetriamine pentaacetic acid (Gd-DTPA) are used as contrast agents in magnetic resonance imaging (MRI) (Shellock and

X.-H. Long (✉) · Q. Liu · G.-H. He
College of Life Science, Shenzhen University, 518060 Guangdong, China
e-mail: longxh006@gmail.com

P.-Y. Yang · J. Yao · Y. Wang
Institute for Biomedical Science, Fudan University, 200232 Shanghai, China

X.-H. Long · G.-Y. Hong · J.-Z. Ni (✉)
Key Laboratory of Rare Earth Chemistry and Physics, Changchun Institute of Applied Chemistry, Chinese Academy of Science, 130022 Jilin, China
e-mail: jzni@szu.edu.cn

Spinazzi 2008; Li et al. 2008). In medicine, gadolinium texaphyrin complex (MGd) is currently subjected to phase III clinical trials for the treatment of brain metastases of nonsmall cell lung cancer (Fricker 2006). Moreover, a wide variety of physiological changes brought about by gadolinium salts are reported. Gadolinium salts are known to inhibit the function of the mononuclear phagocytic system, and have an anticoagulant effect by inhibiting clotting reactions that require calcium (Lee et al. 2004; Liao et al. 2009). The effects of gadolinium salts on the proliferation and apoptosis of some normal and cancer cells have also been studied extensively (Sato et al. 1998; Liu et al. 2006; Fu et al. 2009; Zhang et al. 2009), and these effects related to cell proliferation and apoptosis depend on the concentrations or the types of cells being studied. This suggests that Gd-based treatments have potentials in medical applications in effective therapy of some diseases like cardiac disorders and cancers, and growing interest in the study on the mechanisms of Gd-induced biological effect on cell growth has been aroused. Up to date, the possible molecules and cellular pathways responsible for the promotion and apoptosis of cells induced by Gd-based treatments have been investigated, and the roles of some proteins and cellular processes have been revealed. But the underlying mechanisms are still far from being well elucidated as many more molecules and different cellular pathways are likely involved.

Metabolomics is a "omics" strategy that allows the simultaneous assessment of substrate fluxes within and among different pathways of metabolites under various physiological conditions (Weckwerth 2003; Robertson et al. 2007; Saito and Matsuda 2010). As well known, metabolomic analysis, in contrast to genomics and proteomics that examine the global genes and proteins expression, represents the unbiased distal read-out of the cellular states enabling the generation of meaningful conclusion from the integrative effect of gene expression and protein function. Multiple technologies have been currently used to profile metabolites of the samples in metabolomic researches, including high pressure liquid chromatography (HPLC), nuclear magnetic resonance (NMR) and mass spectrometry (CE/MS, GC/MS, and LC/MS) (Lenz and Wilson 2007; Issaq et al. 2009). Mass spectrometry-based profile, being high throughput, robust, and sensitive, could allow for simultaneous identification of known metabolites as well as characterization of unknown compounds (Bedair and Sumner 2008; Griffiths and Wang 2009). This would meet the challenge for relative insensitivity or for examination of a limited number of metabolites existed for other methods, and has become increasingly popular for metabolomic profiling survey.

In the present study, we have studied the profile change in metabolites released by Hela cells following the treatment with various concentrations of $GdCl_3$ using a high-throughput metabolomic strategy coupling LC to both liner ion trap LTQ Orbitrap and IT TOF MS. This method with enhanced mass resolution, mass accuracy, and detection sensitivity, would allow to investigate the role of metabolites and relevant metabolic processes in different states. Previous study has demonstrated that $GdCl_3$ could inhibit or promote proliferation of several types of cancer cells lines including Hela cells, depending on the concentrations applied (Liu et al. 2006; Zhang et al. 2009). However, the underlying mechanism involved is poorly understood. Additionally, HeLa cell line was found to be more sensitive to Lns than some other cancer cell lines (Shen et al. 2009a). Understanding of Gd-induced cell growth promotion or inhibition would be valuable for development of Lns-based drugs for therapeutic intervention as well as avoiding negative effects. We profiled total 48 metabolites with significant alterations during the cellular responses to the treatment. In combination with multivariate data analysis, we revealed that $GdCl_3$-promoted cell proliferation and progression were characterized by elevated lipid and amino acid metabolisms, indicating an increased utilization of these metabolic intermediates for biosynthetic or energetic purposes. With regard to cells undergone the growth inhibition, down-regulations of lipid, amino acid, and carbohydrate metabolisms, especially down-regulations of metabolites related to the glycolytic and redox pathways were observed. Herein, the study demonstrates that metabolomic information could provide a detailed view of the molecular profiling, and the networks analysis showed that different cell signaling pathways could be triggered by $GdCl_3$ treatment.

Materials and methods

Materials

RPMI 1640 medium was purchased from Gibco (Grand Island, NY, USA). Fetal bovine serum (FBS) was obtained from Hyclone (Logan, UT, USA). Trypsin, trypan blue, standard chemical compounds including haloperidol, diclofenac, verapamil hydrochloride, reserpine, and 3-(4,5-Dimethylthiazoyl-2-yl)-2,5-diphenyltetrazolium bromide (MTT) were from Sigma–Aldrich (St. Louis, MO, USA). Methanol (CH_3OH), chloroform ($CHCl_3$), formic acid (FA), acetonitrile (ACN), and ammonium hydroxide (LC grade) were from Fluka (Buchs & Steinheim, Germany). Penicillin and streptomycin were from Merck (Whitehouse Station, NJ, USA). Other analytical grade chemicals used were from domestic sources. All buffers are prepared with Milli-Q deionized water. $GdCl_3$ solution was prepared by dissolving gadolinium oxide in HCl, evaporating the solution to remove acid, and diluting to different concentrations (0.00075, 0.001, 0.005, 0.01, 0.05, 0.1, 0.5, 1, 1.5, and 2 mM, respectively) to be used in the experiments. Hela, a human cervical carcinoma cell line, was obtained from Shanghai Institute of Biochemistry and Cell Biology, Chinese Academy of Sciences (China).

Cell culture

Hela cells was cultured as previously described (Su et al. 2009). Cells were seeded onto 96-well plates (100 mm^2) at a density of 1×10^6 cells/dish and then incubated for 24 h. $GdCl_3$ treatment was performed by incubating the cells in RPMI 1640 containing 0.5% FBS for 24 and 48 h, respectively, with various concentrations of $GdCl_3$ as stated above. Cell viability was determined using the MTT assay, and trypan blue exclusion. In separate experiments for metabolomic profiling analysis, cells were cultured in the flasks (75 cm^2) with $GdCl_3$ at final concentrations of 0.00075, 0.1, and 2 mM, respectively. Culture media were collected at 24 h after exposure to $GdCl_3$ and extracted using Bligh–Dyer technique as described (Miccheli et al. 1988) and modified by us. Briefly, 1 ml of medium was mixed with 3 ml of cold CH_3OH:$CHCl_3$ (2:1), vortexed for 10 min on ice, followed by centrifugation (Eppendorf, AG, Germany) at 1,4000$\times g$ for 15 min at 4°C. The residue was re-extracted with 2 ml of mixed CH_3OH:$CHCl_3$:H_2O (2:1:1) treated as mentioned above to remove any precipitated proteins. The combined upper (aqueous) phase was evaporated in a SPD1010 speed-vac concentrator (Thermo-Fisher, Milford, MA, USA), re-suspended in 150 µl of water, and then ultrafiltered through a 1,000 Da cut-off filter membrane on a centrifugal filter device (Millipore, Billerica, MA, USA). The extract was lyophilized and reconstructed with mobile phase. All samples were stored at −80°C until use.

MTT assay

The MTT assay was used to evaluate the effect of tested concentrations of $GdCl_3$ on cell growth, as described previously (Situ and Wu 1996). Briefly, 100 µl of a 5 mg/ml MTT stock solution was added to each well of 96-well plate at the end of the treatment time, incubated for 4 h at 37°C. The insoluble formazan product was dissolved in 100 µl of DMSO and the incubation continued for another 30 min at 37°C. Cell growth was assayed by measuring the absorbance of each well at 490 nm using a microplate reader (Tecan, Sunrise, Switzerland) following the equation: Cell growth (%) = (A490 (sample) × 100%/A490 (control) × 100%. Results were expressed as the percentage of the control for cell growth evaluation, with experiments being carried out in triplicate. Cell proliferation as assessed by MTT assay was directly compared to the results from trypan blue exclusion assay, in which cells were counted in triplicate under the optical microscope. All results were presented as the mean ± the standard deviation (SD) for independent experiments, and statistical significance between groups was based on two sided paired Student's t test. $P < 0.05$ was considered as statistically significant.

Liquid chromatography/Mass spectroscopy

Extracts of the metabolites were separated by Liquid chromatography (LC) before Mass spectroscopy (MS) analysis to reduce the sample complexity and thereby enhance the detection sensitivity. To obtain higher separation performance, reversed-phase liquid chromatography (RPLC) and hydrophilic interaction chromatography (HILIC LC) *online* coupled to MS

detection were utilized to cover a larger part of the metabolome. For RPLC separation, a 300 μm inner diameter C_{18} precolumn (LC Packings, San Francisco, CA) was used, where the pre-concentrated and clean-up sample was washed and eluted into a connected *nano*-column (100 mm × 75 μm ID, New Objective Inc., Woburn, MA) filled with 3 μm C_{18} stationary phase. Equal injection volume (50 μl) for the extracts was used and flow rate was 300 nl/min. The gradients for mobile phase (A: 5% ACN/0.1% FA, and B: 100% ACN/0.1% FA) were 5 min at 100% A, 15 min at 5–45% A, and 35 min at 45–95% A, followed by 100% A for another 5 min. For HILIC LC analysis, capillary column XB-NH_2-150 × 2.1 mm with 3 μm particle size (Welch Materials Inc., USA) was used. The gradient and recondition back to the starting condition were done as described above, but mobile solvents were added by 10 mM ammonium acetate (pH 9.1, adjusted with NH_4OH).

Both the IT-TOF (Shimadzu Biotech., Kyoto, Japan) and LTQ-Obitrap (Thermo Electron Corp., USA) MS were applied for monitoring metabolomic patterns. The eluents for LC experiments were electrosprayed into a mass spectrometer for MS analysis and the scan was set for acquisition of both positive and negative ions. Standardizations containing five internal standards in injection solvent were used to assure both chromatographic consistency and internal mass calibrations. Full scan mass spectra were acquired from 50 to 1,000 Da in mass acquisition, followed by MS/MS derived from collision-induced dissociation (CID). For ensuring the reproducibility, three replicate LC–MS measurements were run for each sample, and then the results were exported for further process.

Data processing and metabolomic analysis

Mass spectra data was processed with Xcalibur version 3.2 (Thermo Electron Corp.) and LCMS Solution version 3.10 (Shimadzu Corp.) softwares. Chromatograms were deconvoluted and monoisotopic ion peaks were extracted. XCMS software available from (http://masspec.scripps.edu/xcms/documentation.php) was used to perform background suppression, baseline correction, and data smoothing using default setting. The peaks were aligned and integrated between chromatograms for each ion detected. For metabolites assignment, the Human Metabolome Database (HMDB) (http://www.hmdb.ca/), METLIN metabolite database (http://metlin.scripps.edu/), and Kyoto Encyclopedia of Genes and Genomes (KEGG) ligand database (http://www.genome.jp/kegg/ligand/) were used to determine potentially matching human metabolites consistent with measured accurate masses, elemental compositions, and MS/MS product ions.

To assess the association of significant change in metabolites levels, one-way analysis of variance (ANOVA) and two-tailed *t* test was performed to test for differences in two-sample comparisons or between groups. All mass peak heights were normalized to the peak heights of internal standards (first by summing the total ion current to 10,000) for samples, which is necessary to overcome errors due to the sample loading and the instrument response variation. Measures were run per metabolite on those groups that had detectable expression in at least 20% of the samples. Variations in expression were calculated between data sets (with significance $P < 0.05$ for matched value). The data averaged over the replicate measurements in each sample group was used.

Clustering of class-specific metabolomic patterns was performed using cluster (Eisen et al. 1998) and visualized as heat maps using tree view (Saldanha 2004). Unsupervised hierarchical clustering of samples was accomplished with the use of the log2 transformed and normalized data. Pearson's correlation was used for the similarity metric. In hierarchical clustering, the data were expressed as two-dimensional heat maps of metabolomic signatures using Java TreeView software.

The metabolites that were differentially expressed were mapped to the KEGG biochemical pathways. Mapping of the metabolites to the metabolic pathways used the compound IDs against the IDs as specified in KEGG, followed by search of the relevant pathways and the anabolic and catabolic enzymes for metabolites with variable expressions.

Results

Effect of $GdCl_3$ on Hela cell growth

The effects of $GdCl_3$ on the growth of Hela cells were evaluated by MTT assay, and the results showed that

the status of cell proliferation exhibited a clearly different pattern after incubating in different concentrations of $GdCl_3$ for the different time points. As seen in Fig. 1, the increase in cell growth was observed at lower concentrations of $GdCl_3$ ($\leq$0.5 mM) while the decrease in the growth was found at higher concentrations ($\geq$1 mM) after both 24 and 48 h as compared to the control. The highest percentage for cell proliferation-promoting was 22.4 $\pm$ 1.27% at the concentration of 0.01 mM while the highest percentage for growth suppression was 26.4 $\pm$ 1.03% at the concentration of 2 mM for 24 h treatment. In addition, effect of $GdCl_3$ on cell growth was observed after 48 h of culture. The inhibitory effect was observed at concentrations larger than 1 mM, and the maximum value achieved 64.0 $\pm$ 2.68% of the control on incubation with higher concentration of 2 mM, which was over twofold than that of 24 h treatment at the same concentration. In contrast, the promotional effect was still observed for 48 h with concentrations less than 0.5 mM, but the increase in cell growth was not obvious compared to the 24 h treatment.

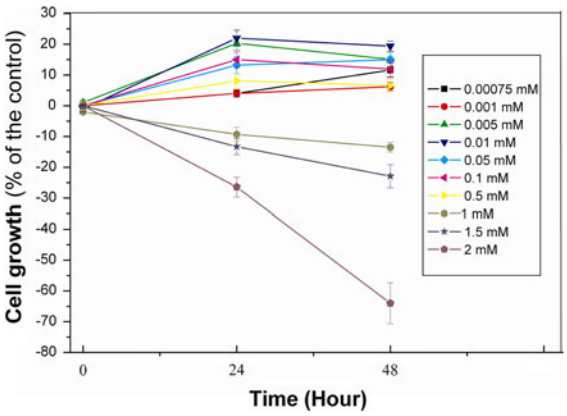

Fig. 1 Effect of $GdCl_3$ on cell growth as determined by MTT assay. HeLa cells were treated with various concentrations of $GdCl_3$ as indicated in "Materials and methods" for 24 and 48 h, respectively, and cells exposed to 0.5% FBS medium only at various time points were used as the controls. The results demonstrated that low concentration of $GdCl_3$ stimulated the cell growth, while relative high concentration of $GdCl_3$ inhibited the growth. Additionally, on incubation with $GdCl_3$ for 48 h, low concentration of $GdCl_3$ (0.00075–0.5 mM) did not markedly increased the cell growth compared to that for 24 h treatment, but high concentration of $GdCl_3$ (concentrations $\geq$1 mM) significantly decreased cell growth. Data were mean $\pm$ standard deviations of triplicate independent determinations. Cell growth was expressed as the percentage of the control

The above results were in good agreement with those obtained by parallel cell counting assay using Trypan Blue exclusion. Morphological feature under phase-inversed microscope also showed the cell growth significantly differed under different $GdCl_3$ treatments. Thus, it can be seen that $GdCl_3$ treatment had either inhibitory or promotional effects on the growth of Hela cells, in concentration- and time-dependent manners.

Extracellular metabolites following $GdCl_3$ treatment

Both lipophilic and hydrophilic LC were utilized for *online* up-front separation to acquire a more comprehensive metabolomic profiling. Figure 2a showed a representative total ion chromatogram (TIC) spectra of *nano*-LC-LTQ Orbitrap for the samples after exposure to $GdCl_3$, and an overlaid pattern of the spectra was shown in Fig. 2b. The results exhibited a significant change in metabolic expression profiles following exposure for 24 h at different concentrations. To reduce between-sample variation and to ensure the reproducibility, three replicate analyses (including biological and technique replicate for each sample) were run. Comparisons across the three measurements (Fig. 3) were evaluated and average correlation coefficients R^2 between two consecutive LC–MS experiments under the identical conditions was greater than 0.95, indicating the reproducibility and reliability of the sample runs in independent replicates.

Metabolite assignments were obtained with accurate mass, elemental composition (mass accuracy $<$10 ppm), and MS–MS fragmentation against the databases. To obtain altered individual "features" observed in various response states, the variables of peak heights were compared (calculated from replicates measures) from the samples with or without $GdCl_3$ treatment. Combined with Multivariate Data Analysis, total 48 metabolites (with $P < 0.05$) were differentially expressed (up or down-regulated, at least twofold variable compared to the control). Listed in Table 1 was the differentially expressed metabolites. Figure 4 displayed an example of extracted ion chromatogram (EIC) of the metabolic intermediate Lysophospholipid following the treatment with

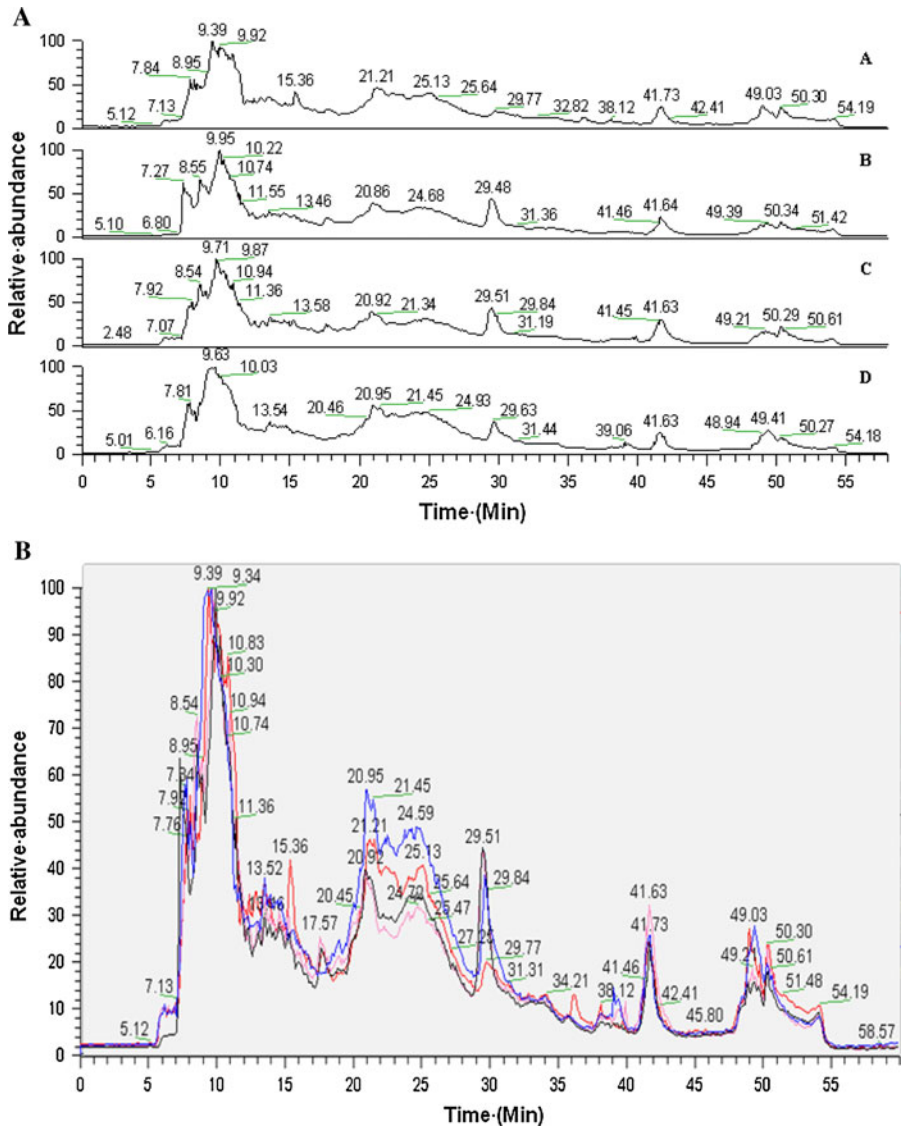

Fig. 2 Representative TIC metabolomic pattern of cells different states using *nano*-LC/LTQ-Obitrap MS. Figure 3a, **a–d** represented profiles of control, 0.00075 mM, 0.1 mM, and 2 mM of $GdCl_3$ respectively, for 24 h treatment. Three replicate analyses were run for each sample. Figure 3b, overlaid pattern of TIC from Fig. 3a, comparison between the samples showed that overall changes in profile were observed following exposure to various concentrations of $GdCl_3$

various $GdCl_3$ concentrations. The up-expressions of the metabolite were observed after treatment with lower $GdCl_3$ concentrations ($\leq$0.1 mM). These metabolites, as listed Table 1, were further mapped to their respective pathways in KEGG, and a detailed information on the metabolite characteristics (such as functional roles, and cellular localization etc.) was contained in Table 2. Hierarchical clustering was used to visualize the relationship of detected changes for metabolites within and between the groups under higher or lower $GdCl_3$ concentrations (Fig. 5). From the overview of identifications of up- or down-regulated metabolites and pathways as specified by KEGG, the differentially expressed metabolites could be grouped into several functional categories, such as lipid metabolism, carbohydrate metabolism, redox homeostasis, and amino acid metabolism etc. The metabolites differentially expressed might represent key regulators for influencing the growth, survival, or progression of Hela cells induced by $GdCl_3$.

Discussion

Global metabolomics as a part of systems biology could allow simultaneous detection of large number of metabolites, and be a useful complement to other "omics" such as transcriptomics or proteomics for

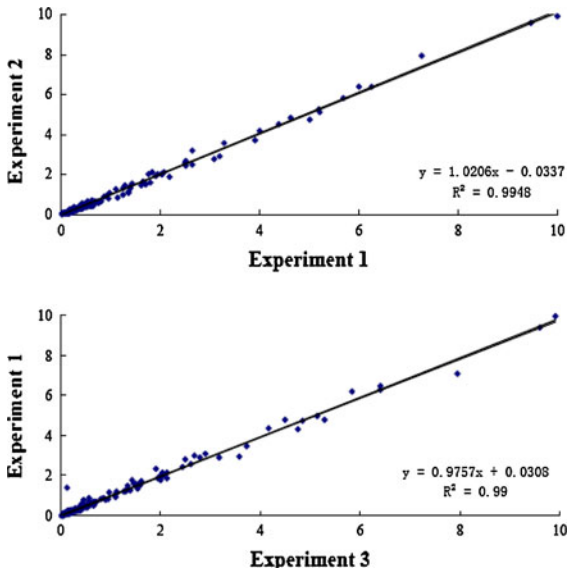

Fig. 3 Reproducibility analysis between consecutive LC–MS runs. Three replicate LC–MS analyses were run for each sample. Each spot represents a pairwise of metabolite with its relative percentage in the sample from the first and second analysis shown on the *x*-axis and the *y*-axis, respectively

characterization of molecules and relevant pathways at given stages for cells, tissues, and organisms. In this work, we utilized the high-throughput LC/MS strategy to investigate the cells extracellular metabolites following $GdCl_3$ incubation at either relatively lower or higher concentrations. The overall changes were observed and a total of 48 metabolites were identified as being changed. These perturbed metabolites, as analyzed by KEGG, could be grouped into several functional categories and involved in different signaling pathways. The involvement of the metabolites implicated the important roles they would play in $GdCl_3$-induced cell growth promotion and inhibition.

A number of lipid-related metabolites were found to be differentially expressed, which were characterized by their generally higher expressions when being treated at lower concentrations while lower expressions at higher concentration of $GdCl_3$. There were some of the metabolites for fatty acid metabolism and energy source, such as lauroyl-CoA, lysoPE, malonylcarnitine, and phosphatidylinositol (PI) etc., that were highly expressed for the faster-growing cells. Some of these are involved in such as fatty acid elongation and transport, and some are phospholipids associated with energy production and cell signaling. For example, lauroyl-CoA and malonylcarnitine are related to the fatty acid elongation, transport, or energy demand (Ushikubo et al. 1996). Phosphatidylinositol is also involved in energy production and is important for signal transduction (Gardocki et al. 2005; Skwarek and Boulianne 2009). These metabolites were up-regulated at lower concentration $GdCl_3$ treatment, suggesting that lipid metabolism for biosynthesis or energetic purpose is active for proliferating cells. Whereas some of the metabolites related to lipid metabolism were down-regulated at higher concentration treatment, suggesting a lower activity for lipid metabolic pathway in viability inhibited cells. Cells under proliferative condition utilize more active substrates to participate physiological processes and to satisfy energy demands than cells under inhibited condition. The enrichments of the intermediates might reflect rapid lipid metabolism turnover for dividing cells, through the use of the metabolites as precursor for synthesis of nucleic acids, proteins, and lipids required for cell proliferation. The variable expression of the lipid-related metabolites demonstrated that $GdCl_3$ could exert different effects on the cells at various concentrations.

Changes in relation to carbohydrate and sugar utilization pathway were observed following incubation of $GdCl_3$ at either lower or higher concentrations. Observably, some of the metabolites related to carbohydrate metabolism were down-expressed after higher concentration $GdCl_3$ treatment. Moreover, a majority of the metabolites belonging to glycolysis for carbohydrate metabolism and ATP synthesis, such as trehalose 6-phosphate, 2-phosphoglyceric acid, and dihydroxyacetone phosphate (DHAP) etc., was detected down-regulated following higher concentration incubation, suggesting a regulatory role of $GdCl_3$ in the metabolic pathway. 2-phosphoglyceric acid, for example, can serve as the substrate in glycolysis through catalyzing the intermediate into phosphoenolpyruvate (PEP) by enolase, which could convert glucose to pyruvate. DHAP, produced from the dehydrogenation of L-glycerol-3-phosphate catalyzed by glycerol 3-phosphate dehydrogenase (GAPDH), is part of the entry of glycerol into the anaerobic glycolytic pathway (Romano and Conway 1996). The observed lower expressions of the metabolites involved in the glycolytic pathway suggested that $GdCl_3$ functions in controlling cell growth by regulating the expressions of these metabolites. It has been proven that in tumor cells there are some protein

Table 1 Differentially expressed metabolites following $GdCl_3$ treatment for 24 h in concentration-depended manner

Metabolite ID[a]	Molecule formula	$GdCl_3$ concentration[c] (mM)		
		0.00075	0.10	2.0
Lipids metabolism[b]				
Lauroyl-CoA	$C_{33}H_{58}N_7O_{17}P_3S$	+	+	–
Malonylcarnitine	$C_{10}H_{17}NO_6$	+		–
LysoPE	$C_{29}H_{60}NO_7P$	+	+	
PI[c]	$C_{41}H_{75}O_{13}P$	+	+	
12a-Hydroxy-3-oxocholadienic acid	$C_{24}H_{34}O_4$		+	
5b-Cholestane-3a,7a,12a,23S,25-pentol	$C_{27}H_{47}O_5$	+		
12-Ketodeoxycholic acid	$C_{24}H_{38}O_4$	–		–
Carbohydrates metabolism				
Trehalose 6-phosphate	$C_{12}H_{23}O_{14}P$			–
2-Phosphoglyceric acid	$C_3H_7O_7P$	–		–
DHAP(10:0)	$C_{13}H_{25}O_7P$			–
N-Acetyl-b-glucosaminylamine	$C_8H_{16}N_2O_5$			–
N-Acetylneuraminic acid	$C_{11}H_{19}NO_9$			+
Cotininegluc uronide	$C_{16}H_{20}N_2O_7$	–		–
5-Methylthioribose 1-phosphate	$C_6H_{13}O_7PS$			
2-(acetylamino)-1,5-anhydro-2-deoxy-3-O-b-D-galactopyranosyl-D-arabino-Hex-1-enitol	$C_{14}H_{23}NO_{10}$			–
1-Phosphatidyl-D-myo-inositol	$C_{11}H_{19}O_{13}P$			–
Peptides and amino Acids metabolism				
L-beta-aspartyl-L-alanine	$C_7H_{12}N_2O_5$	+		
L-alpha-glutamyl-L-hydroxyproline	$C_{10}H_{16}N_2O_6$	–	–	–
Aminomalonic acid	$C_3H_5NO_4$			
Ornithine	$C_5H_{12}N_2O_2$	+		–
Citrulline	$C_6H_{13}N_3O_3$			
Spermidine	$C_7H_{19}N_3$	+		
L-Arginine[c]	$C_6H_{14}N_4O_2$	+		–
Dimethyl-L-arginine	$C_8H_{18}N_4O_2$			–
Hydroxyproline	$C_5H_9NO_3$			+
2-Oxo-4-methylthiobutanoic acid	$C_5H_8O_3S$			–
L-Cystine	$C_6H_{12}N_2O_4S_2$			–
Ophthalmic acid	$C_{11}H_{19}N_3O_6$			–
Glutamylphenylalanine	$C_{14}H_{18}N_2O_5$			–
L-Isoleucine	$C_6H_{13}NO_2$			
Succinylacetone	$C_7H_{10}O_4$			
Nucleic acids metabolism				
Deoxycytidine	$C_9H_{13}N_3O_4$			–
Phosphoribosyl formamidocarboxamide	$C_{10}H_{15}N_4O_9P$	–		
SAICAR	$C_{13}H_{19}N_4O_{12}P$	+		
Xanthylic acid	$C_{10}H_{13}N_4O_9P$	+		
6-Methyladenine	$C_6H_7N_5$	+		–
1,7-Dimethylguanosine	$C_{12}H_{17}N_5O_5$			–

Table 1 continued

Metabolite ID[a]	Molecule formula	$GdCl_3$ concentration[c] (mM)		
		0.00075	0.10	2.0
Vitamins and hormones				
Niacinamide	$C_6H_6N_2O$	–		
N-Methylnicotinamide	$C_7H_8N_2O$			–
Thiamine	$C_{12}H_{17}N_4OS$			–
7-Hydroxy-6-methyl-8-ribityl lumazine	$C_{12}H_{16}N_4O_7$			–
3-Chlorotyrosine	$C_9H_{10}ClNO_3$			–
8-iso-15-keto-PGE2	$C_{20}H_{30}O_5$	–		
Others				
Uroporphyrinogen III[c]	$C_{40}H_{44}N_4O_{16}$	–	–	–
Coproporphyrin III[c]	$C_{36}H_{38}N_4O_8$			–
Portulacaxanthin II	$C_{18}H_{18}N_2O_7$			–
10-formyldihydrofolate	$C_{20}H_{21}N_7O_7$			–
5-Formiminotetrahydrofolic acid	$C_{20}H_{24}N_8O_6$			+
Perillyl alcohol	$C_{10}H_{16}O$			

[a] Metabolites based on searching against Human Metabolome database (HMDB), METLIN, and Kyoto Encyclopedia of Genes and Genomes (KEGG) ligand database

[b] Functional category and metabolic pathway were classified as described under "Materials and methods"

[c] '+' and '−': fold equal or more than two in $GdCl_3$-treated groups versus the control. Evaluated by the peak areas of all features reported by XCMS to detect changes between the two groups. Average data of three replicate experiments was used

enzymes associated with glycolysis, such as different dehydrogenase, enolase, and aldolases etc., are generally overexpressed (Ding et al. 2004; Dos Santos et al. 2004), allowing malignant cells to proliferate and aggress under oxygen deficiency for cells respiration. The development of glycolytic regulation in tumor and proliferating cells is an important strategy for cell growth inhibition since increased glycolysis is frequently seen in cancer cells (Xu et al. 2005). Our data demonstrated that $GdCl_3$ could exhibit the inhibitory effect on cell growth through the pathway related to glycolysis. Furthermore, the variable expressions of the metabolites for glycolytic metabolism indicated that $GdCl_3$ exhibited inhibitory effect through effective intervention of the relevant glycolytic enzymes. It was reported that La^{3+}, one of rare-earth element series, could interact with GAPDH of which the activity can be regulated by Ca^{2+}/Calmodulin (CaM) (Xu et al. 2008). Based on the present results and chemical similarity of Lns series, one might speculate that the target of glycolytic enzymes might be one of the biochemical action of $GdCl_3$, which initiate signaling cascades and play crucial role in regulating cell growth. This might provide a new clue to understand the biological influence of $GdCl_3$ on cell activity. Further functional investigation of the $GdCl_3$-mediated targets would lead to a deeper understanding of the role of $GdCl_3$ in the inhibition of tumor cell proliferation and developing attractive target sites for cancer therapeutics.

Several metabolites that are involved in amino acids metabolic pathway also revealed the increase or decrease in expressions after the treatment. For example, some intermediates involved in arginine, serine, and threonine metabolism displayed the increase in expressions following lower concentration incubation, while those in arginine, and proline or aspartate metabolism pathways showed decreased expressions after higher concentration treatment. The expressions of these peptides or amino acids metabolism-associated metabolites were determined to increase or decrease following the lower or higher concentration treatment, indicating the association of these several metabolites in the inhibitory or promotional effect on Hela cells induced by $GdCl_3$. Moreover, it was interesting to note that some in the glutathione or redox metabolic pathway, such as 2-oxo-4-methylthiobutanoic acid, spermidine, and

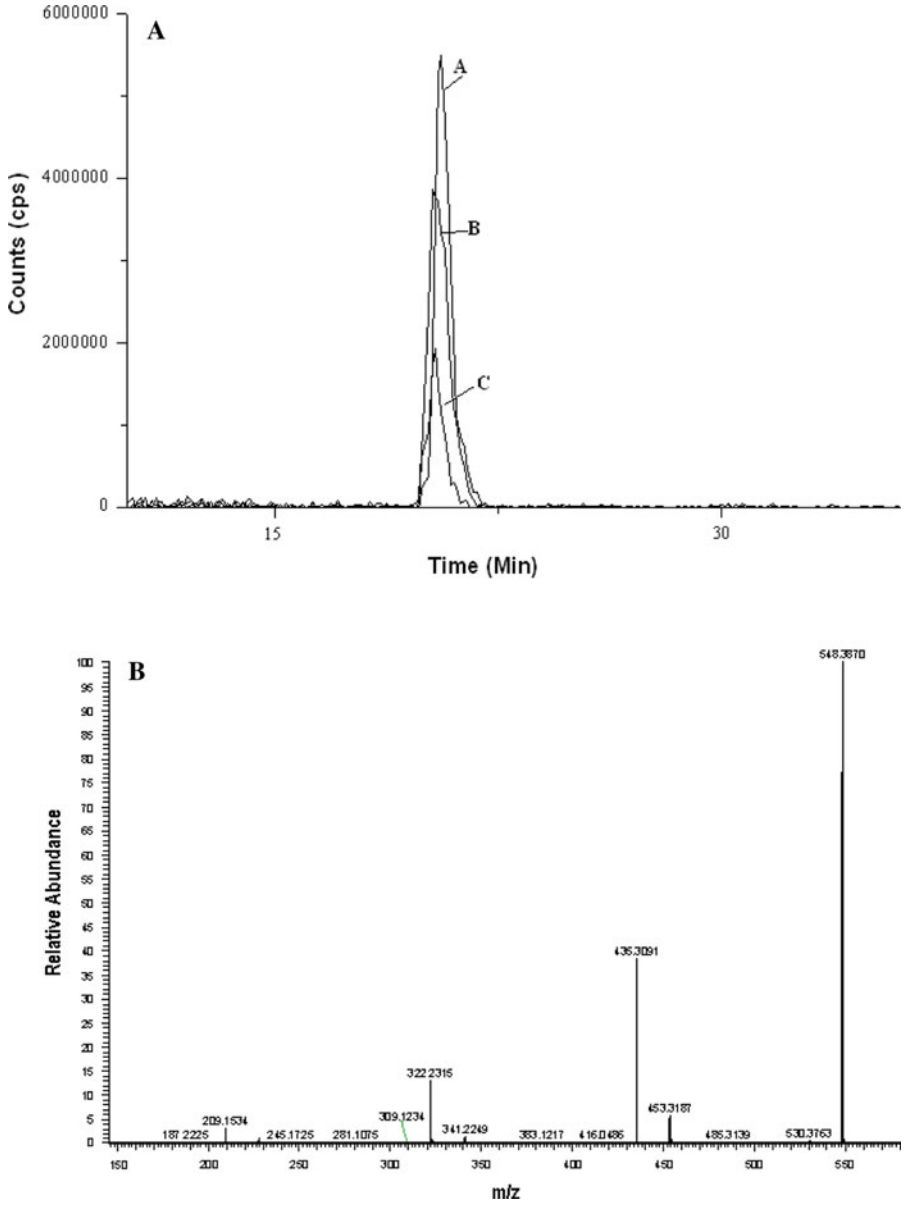

Fig. 4 Typical extracted ion chromatogram (EIC) for metabolite (lysoPE) from the extracts of the different status. **a** direct integration of the EICs. The *symbols A–C* displayed in the EIC corresponded to $GdCl_3$ concentrations of 0.1 mM, 0.00075 mM, and the control, respectively. **b** MS–MS spectrum of the metabolite. The metabolite was considered as differentially expressed with increased or decreased expression (more than twofold, P values <0.05). *cps*, counts/s

ophthalmic acid etc., were detected with decreased levels after higher concentration treatment, suggesting that the redox pathway plays a key role in $GdCl_3$-induced cell growth inhibition. Growing evidence demonstrates that there is a relationship between redox homeostasis/antioxidative system and cell proliferation. Previous studies indicated that glutathione could play a role in maintaining cell redox state and have protective effect against oxidative stress damage (Schafer and Buettner 2001; Vertuani et al. 2004). Reactive oxygen species, such as hydroxyl radical, and hydrogen peroxide etc., generated during metabolism, would lead to cell oxidative injury, and the expressions of some antioxidants such as glutathione and antioxidant enzymes like thioltransferase could reduce or eliminate the freeradicals (Fang et al. 2002). A number of metabolites involved in glutathione pathway and metabolites such as citrullin and arginine with antioxidant capacity showed changed profile, indicating an important role

Table 2 Detailed information about biochemical properties, localization and pathways of differential metabolites

Metabolites	Metabolic pathways[a]	Cellular location[b]	LogP/ hydrophobicity[c]
Lauroyl-CoA	Lipid biosynthesis, fatty acid transport, fatty acid elongation in mitochondria	Cytoplasm; peroxisome	N/1.35
Malonylcarnitine	Fatty acid transport, energy production	Membrane	N/−1.98
LysoPE(0:0/24:0)	Phospholipids, Lipids	Membrane	N/6.79
PI(16:0/16:2(9Z,12Z))	Lipids, phospholipids, membrane component, energy source, cell signaling		N/6.59
12a-Hydroxy-3-oxocholadienic acid	Cholesterols and derivatives, fat solubilization		N/4.3
5b-Cholestane-3a,7a,12a,23S,25-pentol	Steroids and steroid derivatives, hormones, membrane component	Membrane, cytoplasm	N/4.2
12-Ketodeoxycholic acid	Fat solubilization and waste products		N/5.1
Trehalose-6-phosphate	Disaccharide phosphates, starch and sucrose metabolism	Cytoplasm[b]	N/−2.42
2-Phosphoglyceric acid	Glycerophosphates, glycolysis	Cytoplasm	N/−3
DHAP(10:0)	Derivative of dihydroxyacetone phosphate glycolysis metabolic pathway		N/2.0
N-Acetyl-b-glucosaminylamine	Carbohydrates	Cytoplasm[b]	N/−2.52
N-Acetylneuraminic acid	Carbohydrates, nucleotide sugar and amino sugar metabolism	Cytoplasm, lysosome, nucleus	N/−2.78
Cotinineglucuronide	Carbohydrates and carbohydrate conjugates	Cytoplasm[b]	N/−1.57
5-Methylthioribose 1-phosphate	Sugar phosphates, cysteine and methionine metabolism		N/−3.2
1-Phosphatidyl-D-myo-inositol	Sugar phosphates, sugar phosphates; inositol phosphate metabolism		N/−1.66
L-beta-aspartyl-L-alanine	Proteolytic breakdown product of larger proteins		N/3.42
L-alpha-glutamyl-L-hydroxyproline	Dipeptides, breakdown product of collagen		N/−3.49
Aminomalonic acid	Amino acids		N/−3.5
Ornithine	Arginine and proline metabolism; glycine, serine and threonine metabolism	Cytoplasm[b], extracellular, mitochondria	−4.22/−3.64
Citrulline	Alanine and aspartate metabolism, arginine and proline metabolism	Cytoplasm[b], mitochondria	−3.19/−3.27
Spermidine	Arginine and proline metabolism, glutathione metabolism		−0.66/−0.62
L-Arginine	Essential amino acids, alanine and aspartate metabolism, aminoacyl-tRNA biosynthesis	Cytoplasm, extracellular, mitochondria	-4.20/−3.6
Dimethyl-L-arginine	Protein synthesis, amino acid biosynthesis	Cytoplasm[b]	N/−3.15
Hydroxyproline	Arginine and proline metabolism	Cytoplasm, endoplasmic reticulum, mitochondria	−3.17/−3.31
2-Oxo-4-methylthiobutanoic acid	Cysteine and methionine metabolism, glucosinolate biosynthesis	Cytoplasm	N/−0.07
L-Cystine	Amino acids, cysteine and methionine metabolism, ABC transporters	Cytoplasm; extracellular	−5.08/−5.5
Ophthalmic acid	Peptides, analogue of glutathione		N/−3.11
Glutamylphenylalanine	Peptides, gamma-glutamyl derivative	Cytoplasm	N/−4.4
L-Isoleucine	Essential amino acids, aminoacyl-tRNA biosynthesis,	Cytoplasm, extracellular, mitochondria	−1.70/−1.73

Table 2 continued

Metabolites	Metabolic pathways[a]	Cellular location[b]	LogP/ hydrophobicity[c]
Succinylacetone	Valine, leucine and isoleucine biosynthesis	Cytoplasm[b]	N/−0.18
Acetyl-*N*-formyl-methoxykynurenamine	Tyrosine metabolism		−0.158/0.50
Deoxycytidine	Tryptophan metabolism	Extracellular, lysosome, mitochondria, nucleus	N/−1.83
Phosphoribosyl formamidocarboxamide	Purine metabolism, pyrimidine metabolism, pyrimidine metabolism	Cytoplasm[b]	N/−1.82
SAICAR	Biosynthesis from histidine and purine	Cytoplasm	N/−1.95
Xanthylic acid	Biosynthesis of purine nucleotides		−0.18/−0.20
6-Methyladenine	Energy currency, DNA/RNA synthesis, enzyme cofactors, purine metabolism	Cytoplasm	N/−1.77
1,7-Dimethylguanosin	Purines and purine derivatives, nucleosides and nucleoside conjugates		−0.37/−0.45
Niacinamide	Methylated nucleosides	Cytoplasm, extracellular	0.00/−0.21
N-Methylnicotinamide	Component of Nicotinate and nicotinamide metabolism	Cytoplasm[b]	N/−2.11
Thiamine	Essential vitamins	Cytoplasm, membrane, extracellular, mitochondria	N−2.12
7-Hydroxy-6-methyl-8-ribityl lumazine	Riboflavin metabolism, hormones		N/−1.65
3-Chlorotyrosine	Myeloperoxidase-catalyzed oxidation product	Cytoplasm[b]	N/2.5
Uroporphyrinogen III	Porphyrin metabolism	Cytoplasm	N/0.67
Coproporphyrin III	Porphyrin metabolism	Cytoplasm; mitochondria	N/2.53
Portulacaxanthin II	Betaxanthin biosynthesis		N/1.75
10-formyldihydrofolate	One carbon pool by folate	Cytoplasm[b]	N/−1.83
5-Formiminotetrahydrofolic acid	Folate compound	Cytoplasm; extracellular; lysosome; mitochondria	N/−1.26
Perillyl alcohol	Biosynthesis from ornithine, lysine and nicotinic acid	Cytoplasm; extracellular	3.17/2.50

[a] Metabolic pathways derived from KEGG ligand database

[b] Predicted from LogP

[c] Calculated using ALOGPS software (http://www.vcclab.org/lab/alogps/)

for these metabolites in the antioxidant system for high dose $GdCl_3$-treated Hela cells. This suggested that functional control of cellular redox and oxidative defense system pathway might be an important strategy or machinery exhibited by $GdCl_3$. MGd, a gadolinium texaphyrin complex, is regarded as an proapoptotic agent by mediating cellular redox reaction, and is currently subjected to phase III clinical trial for cancer therapy (Hashemy et al. 2006; Fricker 2006). The drug could interfere with the activities of some enzymes such as thioredoxin peroxidases (peroxiredoxins) with redox-active residues, and mediate catalyzed reaction of reducing metabolites such as glutathione, which induce oxidative stress and subsequent apoptosis in tumor cells. Additionally, recent proteomic studies of Hela cell apoptosis induced by Lns salts (such as Yb^{3+} and Gd^{3+}) revealed that some proteins related to redox state and stress resistance, including peroxiedoxin 6, glutathione peroxidase, superoxide dismutase 1, and heat shock proteins, were observed decreased at high concentration (Li et al. 2009; Shen et al. 2009b), which was in agreement with our metabolomic results and demonstrated that the redox and oxidative defense were involved in lanthanide ions-induced cell apoptosis. However, considering that there is a

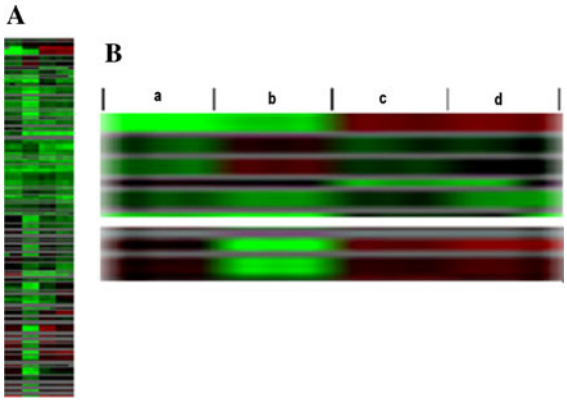

Fig. 5 Heat map representation of unsupervised hierarchical clustering of the sample data. **a** Truncated two-dimensional features of metabolites in given status. The difference in the shade of color represented the difference in expressions of the metabolites. Three technical replicates for each biological group were shown (by *three columns*). **b** Magnified comparison map of **a**. *a–d* respectively represented the different states as described above

similarity/dissimilarity between MGd complex and Gd salts due to common/unique chemical properties, the biological effects on cell growth and the mechanisms of action between them might behave differently. Further understanding the action of Gd complexes and Gd salts would be important for developing Gd-based compounds as drugs and for rational design of new compounds in therapeutic application. The next step is to establish in vivo experiment to verify the results obtained from in vitro cell culture. The favorable cellular response of the treatment demonstrated by in vivo study will be valuable for development of effective therapies by the intervention of targeted biomolecules in treatment of cancers. More studies warrants to be performed and are currently undergone.

Calcium (Ca^{2+}), acting as a ubiquitous second messenger of eukaryotic cells, participates in a large number of signal transduction and regulate cell proliferation, apoptosis, or differentiation (Carafoli 2002). Also Ca^{2+} is believed to play a pivotal role in carcinogenesis and progression (Joseph et al. 2001). Lns ion based on their similarity to Ca^{2+} in ionic radius could replace activating centers of metals such as K^+, Ca^{2+}, Cu^{2+}, or Mg^{2+}, especially Ca^{2+}, which modulate Ca^{2+}-depended enzymatic activities and signal transduction required for cell growth regulation. In our results, as mentioned above, it was found that $GdCl_3$ affected the key enzymes of glycolytic metabolism which require Ca^{2+}-depended CaM regulation. It was reasonable to postulate that Gd^{3+} at a higher concentration could induce Ca^{2+} channel inhibition. As reported, blocking Ca^{2+} entry by Ln ions contributed to the inhibition of cell proliferation of human colon carcinoma cells (Weiss et al. 2001). The biochemical interaction with Ca^{2+} channel by inhibiting the fluxes of intracellular Ca^{2+} might be one of the mechanic action that Gd^{3+} exerted the inhibitory effect on Hela cells. On the other hand, how does Gd^{3+} promote the growth of cells via Ca^{2+} channel or Ca^{2+}-depended signal transduction at lower concentration? Although little information about this is available up to now, induction of cell proliferation by low concentration Ca^{2+} was reported previously (Dai et al. 2008). Based on the chemical/biological similarity of Ln^{3+} to Ca^{2+}, it might be possible that Ln^{3+} functions in cell biological processes, directly or indirectly, through participating in signal transduction mediated by Ca^{2+} (Wang and Yang 2009). For example, Gd^{3+} might interact with Ca^{2+}-depended membrane receptors, such as integrins, G protein-coupled receptor (GPCR), and Ca^{2+} channel, which are potential targets of Ln^{3+}. As a matter of fact, a low concentration of Gd^{3+} can activate membrane receptors on cell surface and initiate downstream signals (Tateyama and Kubo 2006). However, further study is still needed to understand the role of Gd-mediated cell growth proliferation and inhibition.

Those that are associated with nucleic acids metabolism, such as DNA/RNA biosynthesis, purine metabolism, and energy currency etc., were also observed to be regulated following incubation with lower or higher concentrations, suggesting that the metabolites in nucleic acid metabolism were involved in the response to $GdCl_3$ exposure. Results revealed some intermediates such as xanthylic acid, and 6-methyladenine etc., were detected with enhanced expressions following the treatment with lower concentration, whereas 6-methyladenine and 1,7-Dimethylguanosine were significantly under-expressed following the treatment with higher concentration. A high 1,7-Dimethylguanosine (a methylated nucleoside) activity appears to be possibly related with aberrant increase of tRNA methylases activity within tumor tissues (Niwa et al. 1998). Other interesting observations were the differently regulated metabolites involved in other metabolic processes that were essential for cell growth and

development. The altered expressions of the metabolic processes-associated metabolites might reflect the essence and indispensability of these biologically active molecules for cell activity interfered by $GdCl_3$. And involvement of the metabolites in the metabolic pathways might provide potential markers for development of the therapies to inhibit cell malignant proliferation.

In the present work, we have investigated the extracellular metabolomic profile changes of Hela-cell model following conditioned $GdCl_3$ treatments at the system level. A total of 48 metabolites were found to be up or down-expressed ($P < 0.05$) in response to the treatment. The metabolites differentially expressed were involved in different metabolic pathways, such as lipid metabolism, glycolytic pathway, and redox metabolic pathway etc., suggesting that these metabolites altered in the expressions might play a role in $GdCl_3$-mediated cell growth proliferation and inhibition. The observations demonstrated that the untargeted metabolomics could provide a detailed view of a molecular profile, and give some new insights into growth promotion or inhibition of Hela cells regulated by $GdCl_3$. Such results would extend our understanding of the mechanism of tumor cells growth activity perturbed by $GdCl_3$, which in turn could propel the rational exploration and design of Gd-based drugs for development of the treatment of cancers in pharmacological intervention.

Acknowledgments This work was supported by the National Natural Science Foundation of China (No. 20637010). We here thank Dr. Y Wang for helpful review of the manuscript.

References

Bedair M, Sumner LW (2008) Current and emerging mass-spectrometry technologies for metabolomics. Trends Anal Chem 27:238–250

Carafoli E (2002) Calcium signaling: a tale for all seasons. Proc Natl Acad Sci USA 99:1115–1122

Dai J, Li CH, Zhang YZ, Xiao Q, Lei KL, Liu Y (2008) Bioenergetic investigation of the effects of La(III) and Ca(II) on the metabolic activity of Tetrahymena thermophila BF5. Biol Trace Elem Res 122:148–156

Ding SJ, Li Y, Shao XX, Zhou H, Zeng R, Tang ZY, Xia QC (2004) From proteomic analysis to clinical significance: overexpression of cytokeratin 19 correlates with hepatocellular carcinoma metastasis. Proteomics 4:982–994

Dos Santos MD, Borges JBR, Almeida DCG, Curi R (2004) Metabolism of the microregions of human breast cancer. Cancer Lett 216:243–248

Eisen MB, Spellman PT, Brown PO, Botstein D (1998) Cluster analysis and display of genome-wide expression patterns. Proc Nat Acad Sci 95:14863–14868

Fang YZ, Yang S, Wu G (2002) Free radicals, antioxidants, and nutrition. Nutrition 18:872–879

Fricker SP (2006) The therapeutic application of lanthanides. Chem Soc Rev 35:524–533

Fu LJ, Li JX, Yang XG, Wang K (2009) Gadolinium-promoted cell cycle progression with enhanced S-phase entry via activation of both ERK and PI3 K signaling pathways in NIH 3T3 cells. J Biol Inorg Chem 14:219–227

Gardocki ME, Jani N, Lopes JM (2005) Phosphatidylinositol biosynthesis: biochemistry and regulation. Biochim Biophys Acta 1735:89–100

Griffiths WJ, Wang Y (2009) Mass spectrometry: from proteomics to metabolomics and lipidomics. Chem Soc Rev 2009(38):1882–1896

Hashemy SI, Ungerstedt JS, Zahedi H, Avval F, Holmgren J (2006) Motexafin gadolinium, a tumor-selective drug targeting thioredoxin reductase and ribonucleotide reductase. Biol Chem 281:10691–10697

Issaq HJ, Van QN, Waybright TJ, Muschik GM, Veenstra TD (2009) Analytical and statistical approaches to metabolomics research. J Sep Sci 32:2183–2199

Joseph P, Muchnok TK, Klishis ML, Roberts JR, Antonini JM, Whong WZ, Ong TM (2001) Cadmium-induced cell transformation and tumorigenesis are associated with transcriptional activation of c-fos, c-jun, and c-myc proto-oncogenes: role of cellular calcium and reactive oxygen species. Toxicol Sci 61:295–303

Lee CM, Yeoh GC, Olynyk JK (2004) Differential effects of gadolinium chloride on Kupffer cells in vivo and in vitro. Int J Biochem Cell Biol 36:481–488

Lenz EM, Wilson ID (2007) Analytical strategies in metabonomics. J Proteome Res 6:443–458

Li WS, Li ZF, Jing FY, Deng YF, Wei L, Liao PQ, Yang XG, Li XJ, Pei FK, Wang XX, Lei H (2008) Synthesis and evaluation of Gd-DTPA-labeled arabinogalactansas potential MRI contrast agents. Carbohydrate Res 343: 685–694

Li YH, Liu Q, Ni JZ, Liu JJ, Zhou GW (2009) Proteomic study og Gadolinium citrate on Hela cells. J Chin Rare Earths Soc 27:435–440

Liao P, Wei L, Wu H, Li W, Wu Y, Li X, Ni J, Pei F (2009) Biochemical effects of gadolinium chloride in rats liver and kidney studied by ^{1}H NMR metabolomics. J Rare Earths 27:280–287

Liu HX, Yang XD, Wang K (2006) Effects of Lanthanide ions (La^{3+}, Gd^{3+} and Yb^{3+} on growth of human normal liver line 7701 and human cervical carcinoma and the effect of cell apoptosis induced by lanthanide. J Chin Rare Earth Soc 24:484–488

Miccheli A, Aureli T, Delfini M, Di Cocco ME, Viola P, Gobetto R, Conti F (1988) Study on influence of inactivation enzyme techniques and extraction procedures on cerebral phosphorylated metabolite levels by 31P NMR spectroscopy. Cell Mol Biol 34:591–603

Ni JZ (2002) Bioinorganic chemistry of rare earths. Science Press, Beijing

Niwa T, Takeda N, Yoshizumi H (1998) RNA metabolism in uremic patients: accumulation of modified ribonucleosides in uremic serum. Kidney Int 53:1801–1806

Robertson DG, Reily MD, Baker JD (2007) Metabonomics in pharmaceutical discovery and development. J Proteome Res 6:526–539

Romano AH, Conway T (1996) Evolution of carbohydrate metabolic pathways. Res Microbiol 147:448–455

Saito K, Matsuda F (2010) Metabolomics for functional genomics, systems biology, and biotechnology. Annu Rev Plant Biol 61:463–489

Saldanha AJ (2004) Java treeview—extensible visualization of microarray data. Bioinformatics 20:3246–3248

Sato TM, Hashizume M, Hotta Y, Okahata Y (1998) Morphology and proliferation of B16 melanoma cells in the presence of lanthanoid and Al ions. Biometals 11:107–112

Schafer FQ, Buettner GR (2001) Redox environment of the cell as viewed through the redox state of the glutathione disulfide/glutathione couple. Free Radic Biol Med 30: 1191–1212

Shellock FG, Spinazzi A (2008) MRI safety update 2008: part 1. MRI contrast agents and nephrogenic systemic fibrosis. AJR Am J Roentgenol 191:1129–1139

Shen LM, Lan ZY, Liu Q, Ni JZ (2009a) Apoptosis of cancer cells induced by lanthanum citrate. J Chin Rare Earths Soc 27:441–446

Shen LM, Liu Q, Ni JZ, Hong GY (2009b) A proteomic investigation into the human cervical cancer cell line HeLa treated with dicitratoytterbium (III) complex. Chem Biol Interact 181:455–462

Situ ZQ, Wu JZ (1996) Cell culture. World Book Press, Xi-an

Skwarek LC, Boulianne GL (2009) Great expectations for PIP: phosphoinositides as regulators of signaling during development and disease. Dev Cell 16:12–20

Su XE, Zheng XN, Ni JZ (2009) Lanthanum citrate induces anoikis of Hela cells. Cancer Lett 285:200–209

Tateyama M, Kubo Y (2006) Dual signaling is differentially activated by different active states of the metabotropic glutamate receptor 1alpha. Proc Natl Acad Sci USA 103:1124–1128

Ushikubo S, Aoyama T, Kamijo T, Wanders RJ, Rinaldo P, Vockley J, Hashimoto T (1996) Molecular characterization of mitochondrial trifunctional protein deficiency: formation of the enzyme complex is important for stabilization of both alpha- and beta-subunits. Am J Hum Genet 58:979–988

Vertuani S, Angusti A, Manfredini S (2004) The antioxidants and pro-antioxidants network: an overview. Curr Pharm Des 10:1677–1694

Wang K, Yang XG (2009) Safety issues of lanthanide-based compounds as diagnostic and therapeutic agents as viewed from cellular inorganic chemistry. Prog Chem 21:803–818

Weckwerth W (2003) Metabolomics in systems biology. Ann Rev Plant Biol 54:669–689

Weiss H, Amberger A, Widschwendter M, Margreiter R, Ofner D, Dietl P (2001) Inhibition of store-operated calcium entry contributes to the anti-proliferative effect of non-steroidal anti-inflammatory drugs in human colon cancer cells. Int J Cancer 92:877–882

Xu RH, Pelicano H, Zhou Y, Carew JS, Feng L, Bhalla KN, Keating MJ, Huang P (2005) Inhibition of glycolysis in cancer cells: a novel strategy to overcome drug resistance associated with mitochondrial respiratory defect and hypoxia. Cancer Res 65:613–621

Xu K, Yang XD, Wang K (2008) La3+ induced binding of Calmodulin (CaM) to CaM-binding proteins in rat brain homogenate. Chem J Chinese Univ 29:2525–2530

Zhang Y, Fu LJ, Li JX, Yao XG, Yao XD, Wang K (2009) Gadolinium promoted proliferation and enhanced survival in human cervical carcinoma cells. Biometals 22:511–519